IOP Publishing Mater. Res. Express 5 (2018) 045702 https://doi.org/10.1088/2053-1591/aab907

Materials Research Express

RECEIVED
15 December 2017

REVISED
3 January 2018

ACCEPTED FOR PUBLICATION
23 March 2018

PUBLISHED
13 April 2018

PAPER

Hemispherical cavities on silicon substrates: an overview of micro fabrication techniques

O Poncelet[1,2], J Rasson[1], R Tuyaerts[2], M Coulombier[2], R Kotipalli[1], J-P Raskin[1] and L A Francis[1]

[1] Institute of Information and Communication Technologies, Electronics and Applied Mathematics, Université catholique de Louvain, Place du Levant, 3, 1348 Louvain-la-Neuve, Belgium

[2] Institute of Mechanics, Materials, and Civil Engineering, Université catholique de Louvain, Place Sainte Barbe, 2, 1348 Louvain-la-Neuve, Belgium

E-mail: olivier.poncelet@uclouvain.be

Keywords: bio-inspired hemispherical cavities, micro fabrication, colloids, polarization, XeF_2 dry etching, HNA wet etching, electrochemical etching

Abstract

Hemispherical photonic crystals found in species like *Papilio blumei* and *Cicendella chinensis* have inspired new applications like anti-counterfeiting devices and gas sensors. In this work, we investigate and compare four different ways to micro fabricate such hemispherical cavities: using colloids as template, by wet (HNA) or dry (XeF_2) isotropic etching of silicon and by electrochemical etching of silicon. The shape and the roughness of the obtained cavities have been discussed and the pros/cons for each method are highlighted.

1. Introduction

Hemispherical cavities are macroscopic optical structures found in many species of lepidopteran and coleopteran. Most especially, the *Papilio* family, such as the *Papilio blumei* [1, 2], the *Papilio palinurus* [3], the *Papilio ulysse* [4] or the *Papilio peranthus* [5, 6] are known to exhibit hemispherical-like photonic crystal, as well as some coleopteran such as the *Calidea panaethiopica* [7], *Chlorophila obscuripennis* [8] or the *Cicindella chinensis* [9] and *repanda* [10]. This characteristic photonic structure has been widely studied for its optical applications: colour and colour mixing [11–16] and polarization effects [9, 17, 18]. Most recently, the *blumei* structure was even studied for its gas sensing properties [19, 20]. The hemispherical shape is also used in many other optical applications, such as shell resonator [21, 22], electro-wetting lens [23], micromirror [24] and optomechanical accelerometer [25] or in polymer chemistry to confine block copolymers [26, 27].

In this work, we investigate and compare four different methods to micro fabricate hemispherical cavities onto silicon substrates using fabrication techniques. The first method is widely used to fabricate hemispherical cavities and consists of using self-assembled films of spherical colloids as a template or a mold. Sol-gel coating [28–31], electrodeposition [18, 32, 33] or e-beam [2] are then used to fill the colloid interstitial spaces to form hemispherical cavities. The three other methods consist of an isotropic etching of the silicon by: $HF:HNO_3:CH_3COOH$ solution (namely HNA) [9] mostly used to etch large cavities [23, 25], XeF_2 gas used in MEMS releasing processes [34–38] and electrochemical etching used to fabricate concave porous silicon structures [20]. The methods investigated here allow to fabricate a wide range of cavity sizes with different degrees of surface roughness.

For each method, recipes and procedures are fully described. The fabricated cavities are analyzed in term of their curvature quality thanks to cross-section and top-view scanning electron microscope (SEM) observation. In fact, it remains challenging to etch perfect hemispherical cavities in a crystalline material like silicon. We then show a quantitative method to control if the surface quality of a cavity is specular or not, which is mandatory for most optical applications.

© 2018 IOP Publishing Ltd

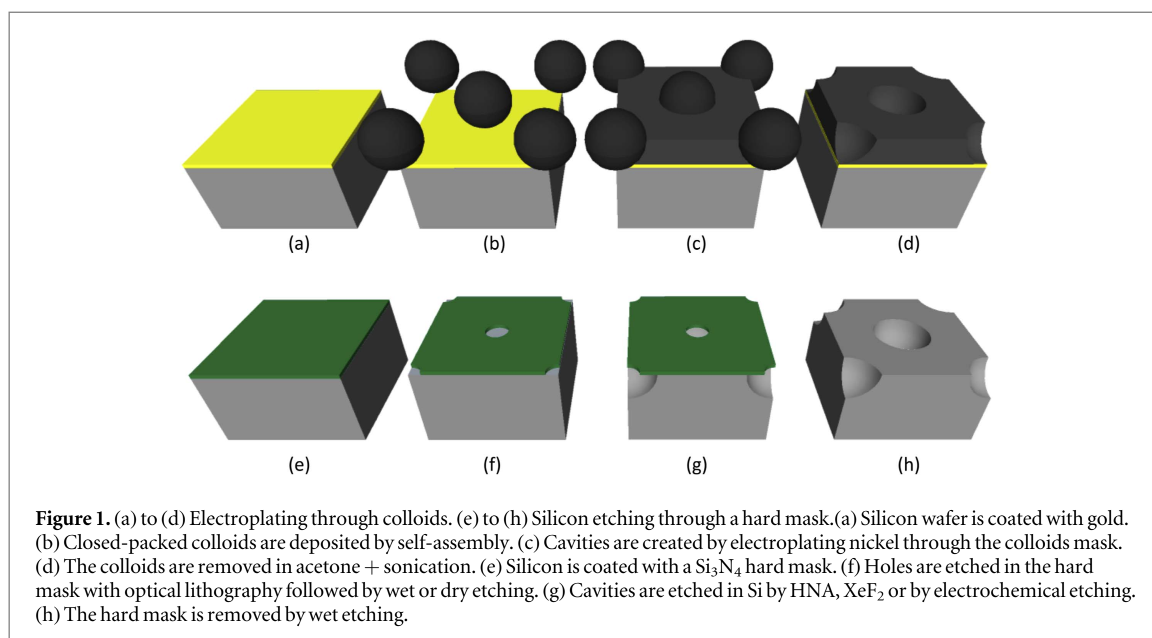

Figure 1. (a) to (d) Electroplating through colloids. (e) to (h) Silicon etching through a hard mask.(a) Silicon wafer is coated with gold. (b) Closed-packed colloids are deposited by self-assembly. (c) Cavities are created by electroplating nickel through the colloids mask. (d) The colloids are removed in acetone + sonication. (e) Silicon is coated with a Si_3N_4 hard mask. (f) Holes are etched in the hard mask with optical lithography followed by wet or dry etching. (g) Cavities are etched in Si by HNA, XeF_2 or by electrochemical etching. (h) The hard mask is removed by wet etching.

2. Materials and methods

Substrates used for the fabrication of cavities via the use of colloids, HNA etching and XeF_2 are 3 inches CZ p-type boron doped silicon wafers with a $\langle 100 \rangle$ orientation and 10–20 $\Omega \cdot$ cm resistivity range (Siegert Wafer, Germany) while the electrochemically etched cavities were fabricated using CZ p^+-type heavily boron doped wafers with a $\langle 100 \rangle$ orientation and presenting a resistivity range of 0.8–1.2 m$\Omega \cdot$ cm (Sil'tronix Silicon Technologies, France). Before any processing, all wafers were cleaned with piranha solution (H_2SO_4 9597%: H_2O_2 30%, 5:2 v/v) for 10 min, followed by a rinsing in deionized water then a 15 s immersion in a 2% HF solution and a final rinsing in deionized water.

2.1. Cavities with colloids

Cleaned silicon substrates were coated with a 100 nm-thick gold film by e-beam evaporation and were then cut in 1×1 cm^2 samples (figure 1(a)). Those samples were exposed to a plasma oxygen to render the surface hydrophilic, mandatory for the next step. Close-packed hexagonal colloidal monolayers were transferred on the samples by using a liquid interface-mediated surface protocol (direct assembly, figure 1(b)) [39–42]. Aqueous suspensions of sulphonate polystyrene colloidal particles with a diameter of 2.4 μm and 6 μm were used as the source of colloids.

Nickel was then electrochemically grown through the interstitial spaces between colloids [18] to obtain hemispherical cavities of 2.4 μm or 6 μm (figure 1(c)). A $NiSO_4(H_2O)_6/H_3BO_3$ solution and a platinum electrode were used. The potential was set at −1 V. The electro-plating must be stopped when the nickel reaches half of the colloids height. This can be done by following the real-time current signal and by switching the potential off when the current reaches a minimum (figure 2). Indeed, after a transition period the current decreases because the contact area between the electrolyte and the substrate decreases while the nickel grows. At the mid-height, the contact area reaches its minimum then starts to increase. Above this point, the colloids become gradually encapsulated in nickel and will be difficult to remove. Colloids were then removed with ultrasonication in an acetone bath (figure 1(d)).

2.2. Cavities by HNA etching

Silicon substrates were coated with a 150 nm-thick LPCVD Si_3N_4 (figure 1(e)). This coating method is used because Si_3N_4 sustains a tensile stress which makes it suitable to be under-etched. A hexagonal pattern of 1 μm holes and 16 μm spacing was etched by optical lithography followed by a reactive ion etching step (RIE) with SF_6 (figure 1(f)). Hemispherical cavities were then etched through those holes by means of HNA (figure 1(g)), an isotropic etchant composed of fluorhydric acid (HF 49%), nitric acid (HNO_3 70%), and glacial acetic acid (CH_3COOH 99100%). We used a 3:94:3 composition in volume at room temperature and under stirring. Small amounts of HF and CH_3COOH ensure a smoothly etched surface and a slow etch rate [43–45]. A slow etch rate is mandatory here to avoid coalescence of the cavities. The nitride layer was then removed with phosphoric acid (H_3PO_4) at 180 °C (figure 1(h)).

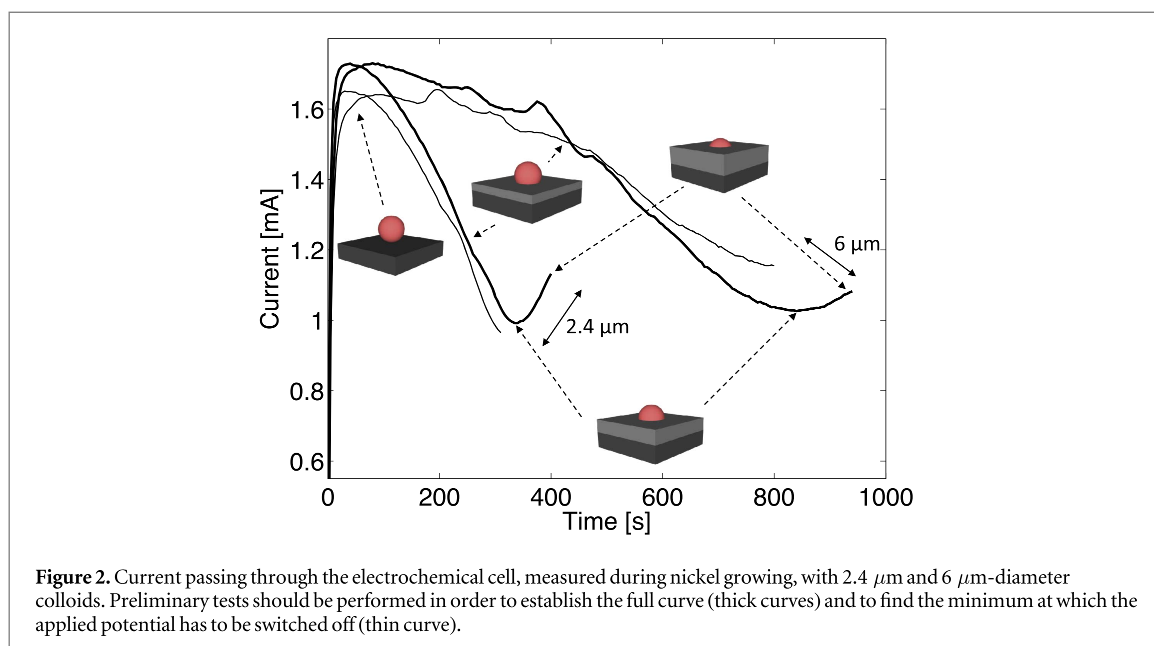

Figure 2. Current passing through the electrochemical cell, measured during nickel growing, with 2.4 μm and 6 μm-diameter colloids. Preliminary tests should be performed in order to establish the full curve (thick curves) and to find the minimum at which the applied potential has to be switched off (thin curve).

In order to analyse the cavities from their rear side, membranes composed of these cavities have been fabricated. Silicon cavities were oxidized (300 nm) in a thermal process (H_2O at 950 °C). A lithography is then performed on the rear side of the samples to open the SiO_2 in square windows.

A thick protect-resist was applied on the front surface by spin-coating in order to fill the cavities, to protect the front SiO_2 and to mechanically support the membrane. The membranes were then released by etching the silicon through the rear mask with TMAH. The resulting membranes consist in SiO_2 cavities supported by a thick resist.

2.3. Cavities by XeF_2 etching

The cavities were etched by xenon fluoride (XeF_2) in a Xactix e1 chamber (SPTS) through the procedure applied for HNA etching (figures 1(e) to (h)). The samples were dipped in HF 2% during 10 s, rinsed and finally placed in a 120 °C oven during 5 min before the next step. XeF_2 was injected in the etching chamber at 3 Torr. The gas was kept in the chamber for 5 s and was pumped out. The exposure time is limited to 5 s to ensure a high selectivity between the silicon etching and the nitride hard mask etching, by limiting the by-product (which etch the nitride) staying in the chamber. This cycle was then repeated 10 times. Tests were conducted on 1 $\times$ 1 cm^2 dies.

2.4. Cavities by electrochemical etching

The wafers were submitted to the same process as described earlier for the XeF_2 and HNA etching (figures 1(e) to (h)). Following the silicon nitride opening, the samples were electrochemically etched in a custom-made Teflon etch cell with a potentiostat (Metrohm) as the current source, the wafer as the working electrode and a platinum coil as the counter-electrode.

The electrolyte used for the electrochemical etching of porous silicon is a 3:1 (v/v) solution of 49 % HF and absolute ethanol. The current is fixed to have an initial current density of 200 mA cm^{-2} and was applied for 10 min to obtain a porous silicon hemispherical cavity. A long etching time is required since the etch rate is directly linked to the current density at any point in time. For the etching of a 3D structure, such as a cavity, the total surface to etch continuously increases over time, which leads to a decrease of the effective current density at the etching interface and incidentally of the etching rate. Following the porosification, the silicon nitride layer was chemically etched by immersing the samples in a highly concentrated HF solution, then rinsing them in isopropanol before removing the porous silicon in a 2 M KOH solution and successively rinsing the samples in deionized water and 2-propanol then drying them under a flow of dry nitrogen.

3. Results

3.1. Colloids method

The first limitation of using colloids to create a self-assembled monolayer is their diameters. The small particles (2.4 μm) tend to easily assemble in a hexagonal close-packed film (figure 3(a)) while it takes much more effort to achieve the same results with the large particles (6 μm, figure 3(b)). From a macroscopic point of view

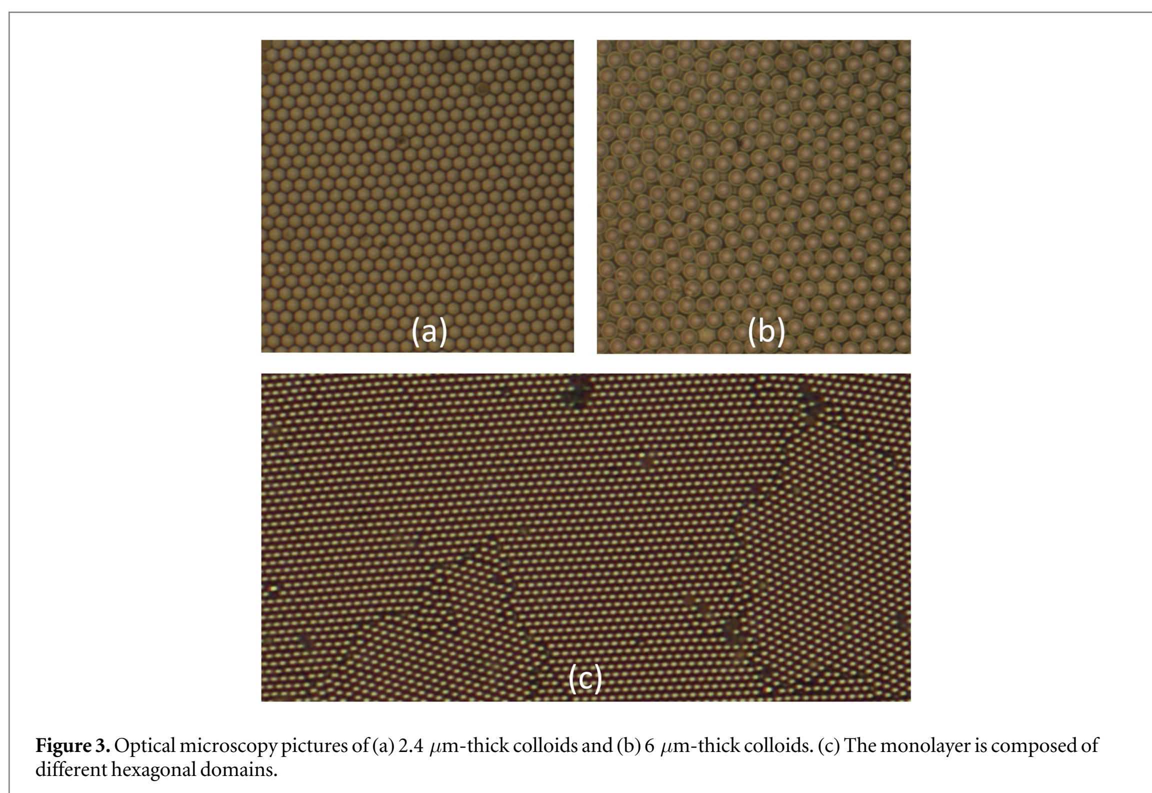

Figure 3. Optical microscopy pictures of (a) 2.4 μm-thick colloids and (b) 6 μm-thick colloids. (c) The monolayer is composed of different hexagonal domains.

(figure 3(c)), both films arrange themselves in a polycrystalline network. Standard defects such as grain joints and stacking problems then appear as it is the case at the atomic scale in any polycrystalline materials (figure 3(c)).

Scanning electron microscopy (SEM) after the electrochemical step shows that the colloids sustained well the nickel growing and the electrolyte (figures 4(a) and (b)). Both colloids size stay in the hexagonal network (figures 4(c) and (d)) and adhere to the substrate, allowing the nickel to be shaped in the expected hemispherical geometry (figures 4(e) and (f)). This is confirmed by the top-view, showing perfect circle cavities (figure 4(g)).

The 2.4 μm-colloids used here are easily dissolvable in acetone and thus can be easily removed from the nickel cavities. On the other hand, the 6 μm-colloids are composed of cross-linked polymers which makes them difficult to dissolve in acetone (figure 4(g)). A longer sonication time is thus needed.

Smaller colloids as well as other metal plating (like copper) can be used, depending on the application.

3.2. HNA etching method

Getting hemispherical cavities by wet etching is a very convenient method because it doesn't require any manual steps compared to the colloid method. Moreover, the optical lithography allows the fabrication of perfect networks of cavities without any defects (figures 5(a) and (b)). However, due to the nature of the wet etching, caution must be paid to avoid cavities coalescence (figures 5(c) to (e)). When it happens, cavities are quickly smoothed out leading to the loss of the hemispherical shape (figures 5(f) to (h)). HNA is in fact a well-known solution to chemically smooth rough surfaces or to thin silicon wafers. In contrast to a thinning process, etching 3D-cavities implies that the etch-rate varies with the size of the cavities because the surface of the etch-front continuously increases during the process. It is also more and more difficult for the fresh solution to diffuse through the holes in the hard mask (figure 5(d)), and for the by-product of the etching to be evacuated out of the cavities. The etch-rate is thus difficult to measure but started at around 3 μm/min and decreased progressively.

The cavities obtained by HNA etching are not fully-hemispherical (figures 5 and 6). In fact, top-view and cross-section of the cavities (figures 5(d) and (e)) clearly show a rounded square-shape where it should be a perfect circle. In fact, the wagon-wheel diagram [46] of the HNA used here shows a small degree of anisotropy (figure 7). The etch-rate in the [100] direction is faster than the etch-rate in the [110] direction and thus leads to visible anisotropic effects (figure 6).

Crystalline plans and directions are depicted in figure 6 in two ways in order to highlight the anisotropic effets. On many pictures in figures 5 and 6, a triangular shape is observed. From figure 6, it is clear that this shape is formed from the edges between the {111} and {100} family plans, and {111} and {110}. However, it should be noted that the triangle is not exactly the {111} plan. Cross-section of the cavities (figures 5(c), (e) and (f)) as well as the back of the cavities membrane (figures 5(i) and 6(e)) show a curved shape more than a fully flat plan.

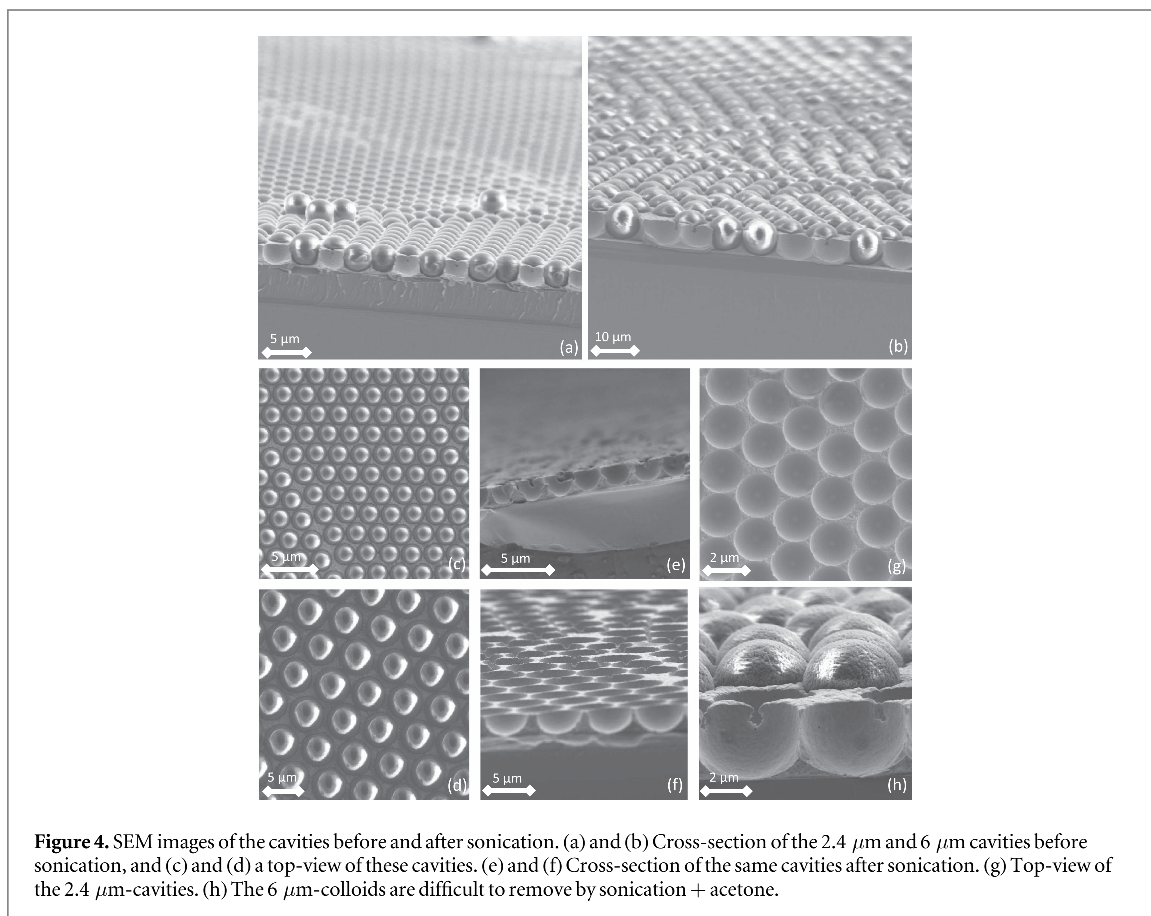

Figure 4. SEM images of the cavities before and after sonication. (a) and (b) Cross-section of the 2.4 μm and 6 μm cavities before sonication, and (c) and (d) a top-view of these cavities. (e) and (f) Cross-section of the same cavities after sonication. (g) Top-view of the 2.4 μm-cavities. (h) The 6 μm-colloids are difficult to remove by sonication + acetone.

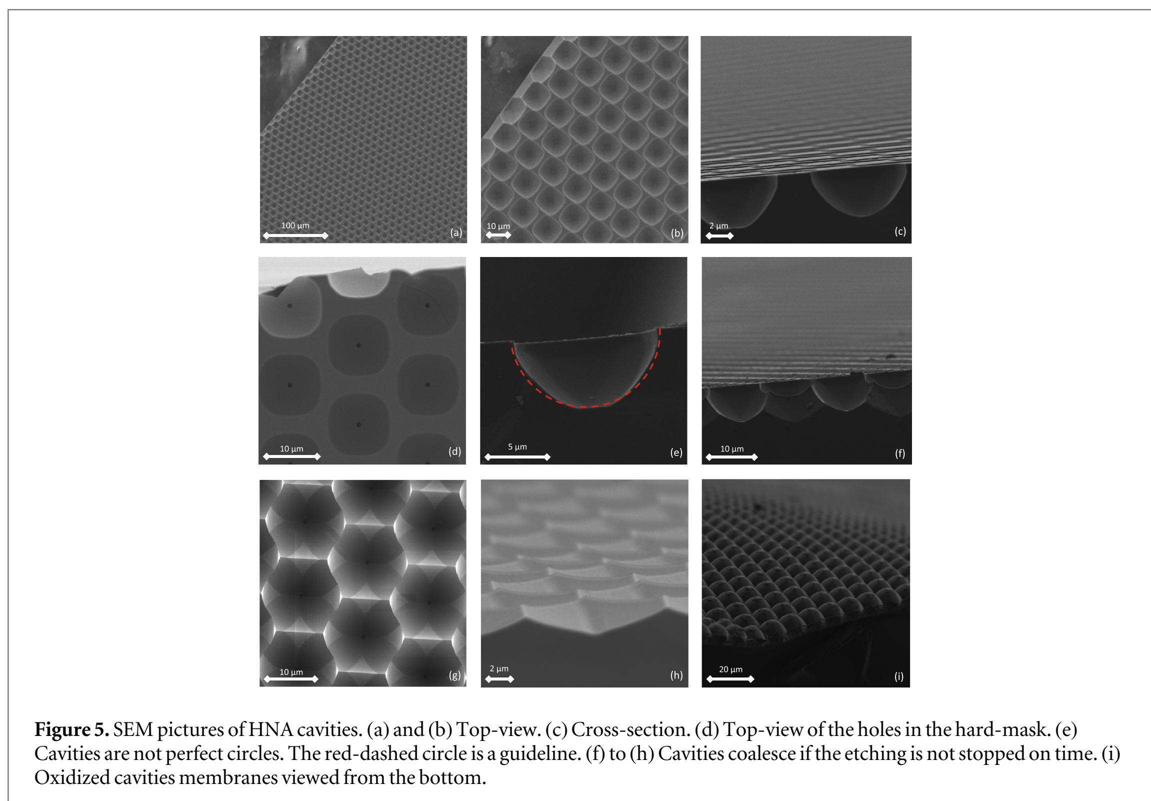

Figure 5. SEM pictures of HNA cavities. (a) and (b) Top-view. (c) Cross-section. (d) Top-view of the holes in the hard-mask. (e) Cavities are not perfect circles. The red-dashed circle is a guideline. (f) to (h) Cavities coalesce if the etching is not stopped on time. (i) Oxidized cavities membranes viewed from the bottom.

In some cavities (figures 5(g) and 6(b), (c) and (f)), edges between {110} plans divided the cavities in four parts. Finally, even if the silicon is etched through circular holes (figure 5(d)), the bottom of the cavities remains flat and squared, exactly as the (00–1) plan in the 3D schematic of figure 6.

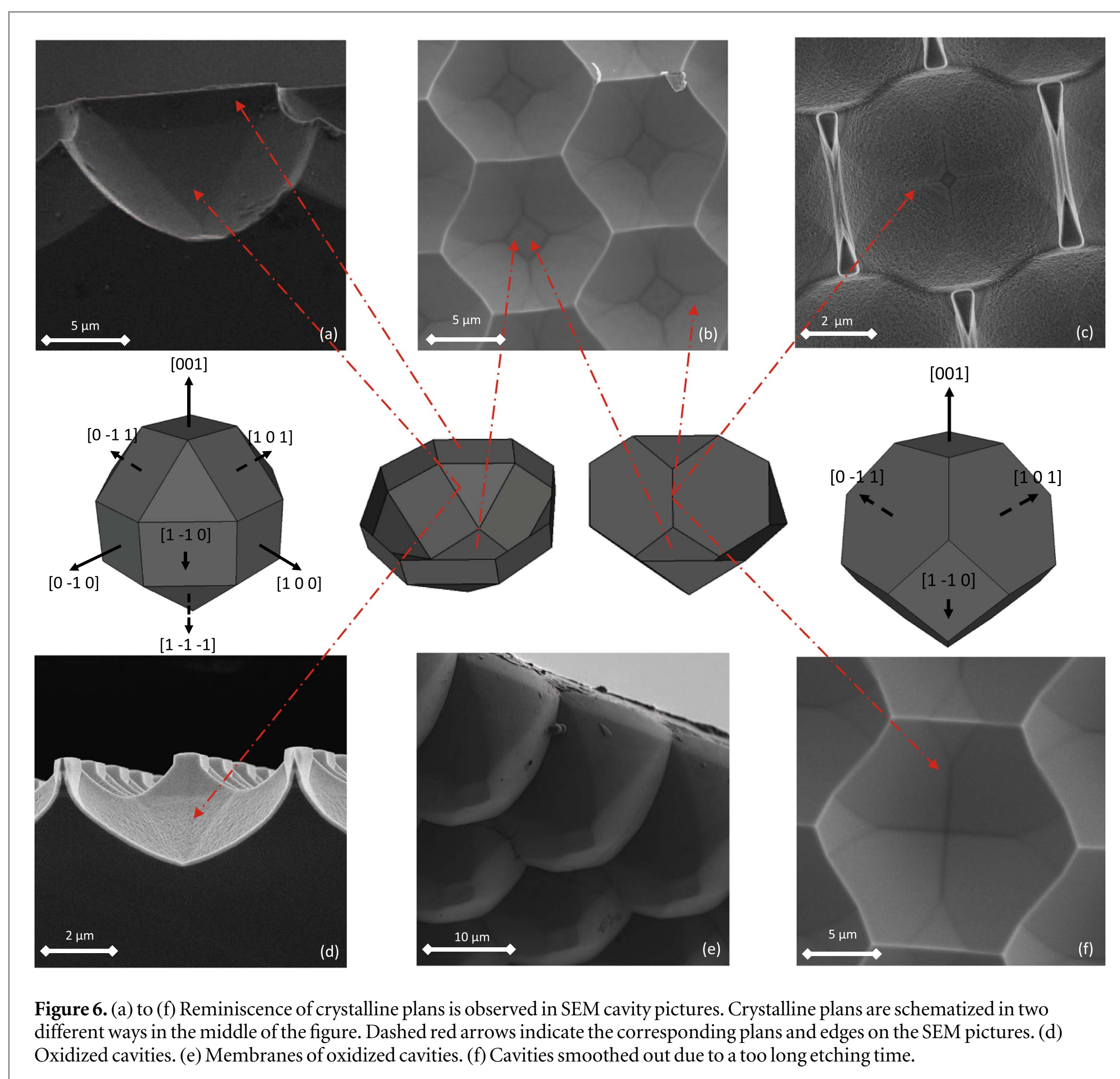

Figure 6. (a) to (f) Reminiscence of crystalline plans is observed in SEM cavity pictures. Crystalline plans are schematized in two different ways in the middle of the figure. Dashed red arrows indicate the corresponding plans and edges on the SEM pictures. (d) Oxidized cavities. (e) Membranes of oxidized cavities. (f) Cavities smoothed out due to a too long etching time.

Despite the reminiscence of the crystalline plans, the cavities are still mainly hemispherical, as shown by the cross-section in figures 5 and 6.

HNA is more suitable for large cavities (radius >2 μm) because an isotropical etch front takes time to establish as the etching starts from a flat surface. However, the cavities can be etched through the whole wafer thickness [23].

3.3. XeF_2 etching method

Cavities fabricated with XeF_2 are perfectly hemispherical (figure 8) but the surface roughness of those cavities is important (figures 8(b) and (c)). The roughness can be reduced afterward by dipping the sample in a soft HNA solution for a few seconds. In this case a 45 s immersion in a 6:88:6 v/v HNA solution was used (figure 8(d)). A longer HNA step will further smooth out the surface but will increase the size of the cavities. It becomes less interesting as the aim of dry etching is to avoid chemicals.

The XeF_2 etching has the advantage to be done in a transparent chamber. The under etching can thus be controlled *in situ* with an optical microscope, allowing the process to be stopped before the cavities coalescence. As it is the case with HNA, very large cavities can be fabricated with this technique but it will require a large amount of pulses as the etch-front surface continuously increases.

3.4. Electrochemical etching method

Cavities obtained by electrochemical etching of silicon are not fully hemispherical (figure 9). Cross-section view of a cavity shows a slight asymmetric deviation from a perfect circle (figure 9(a)). A small roughness is observed on the surface of the cavities after the porous silicon removal by KOH etching (figure 9(b)). From the top view (figure 9(c)), we observe that the technique is not fully isotropic and results in a rounded-square shape, which is similar to what is observed with HNA etching. The squared cavities indicate that the etch rate is not equal in all

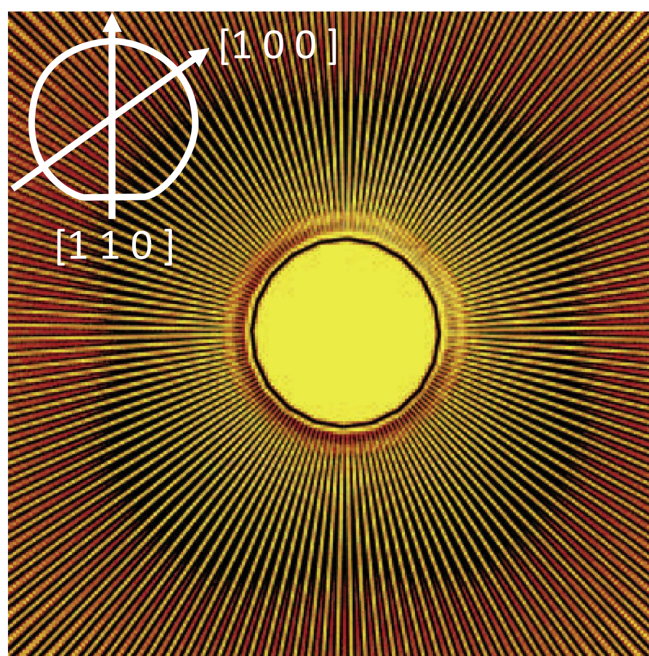

Figure 7. Wagon wheel of 3:94:3 HNA etchant. Contour of the black area shows that the etching is not perfectly isotropic, i.e. a perfect circle. The above left-corner insert shows the crystalline directions of the wafers used in this work.

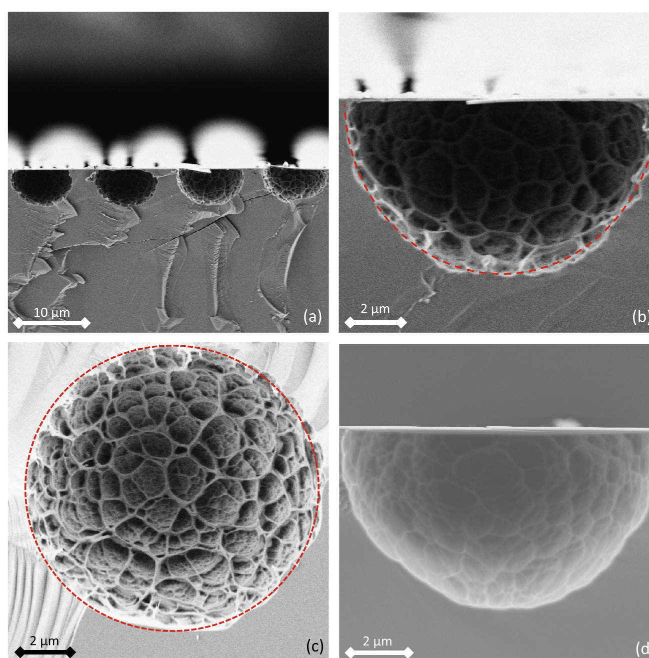

Figure 8. Cavities etched by XeF_2. (a) Cross-section of cavities and (b) zoom on a single cavity. (c) Top-view of a cavity. (d) Smoothed cavity after HNA etching. The red-dashed lines in (b) and (c) are guide-lines to control the isotropicity.

the directions. This method is more adapted to produce small cavities ($<10\ \mu$m). In fact, the current needed is high and the etch rate quickly decreases monotonically.

3.5. Optical characterisation

Smoothness and curvature-quality of the cavities were checked under an optical microscope with a cross-polarizer (perpendicular configuration of two linear polarizers). This polarizer configuration allows the observation of back-reflected light which has sustained any polarization rotations after a reflection. Basically,

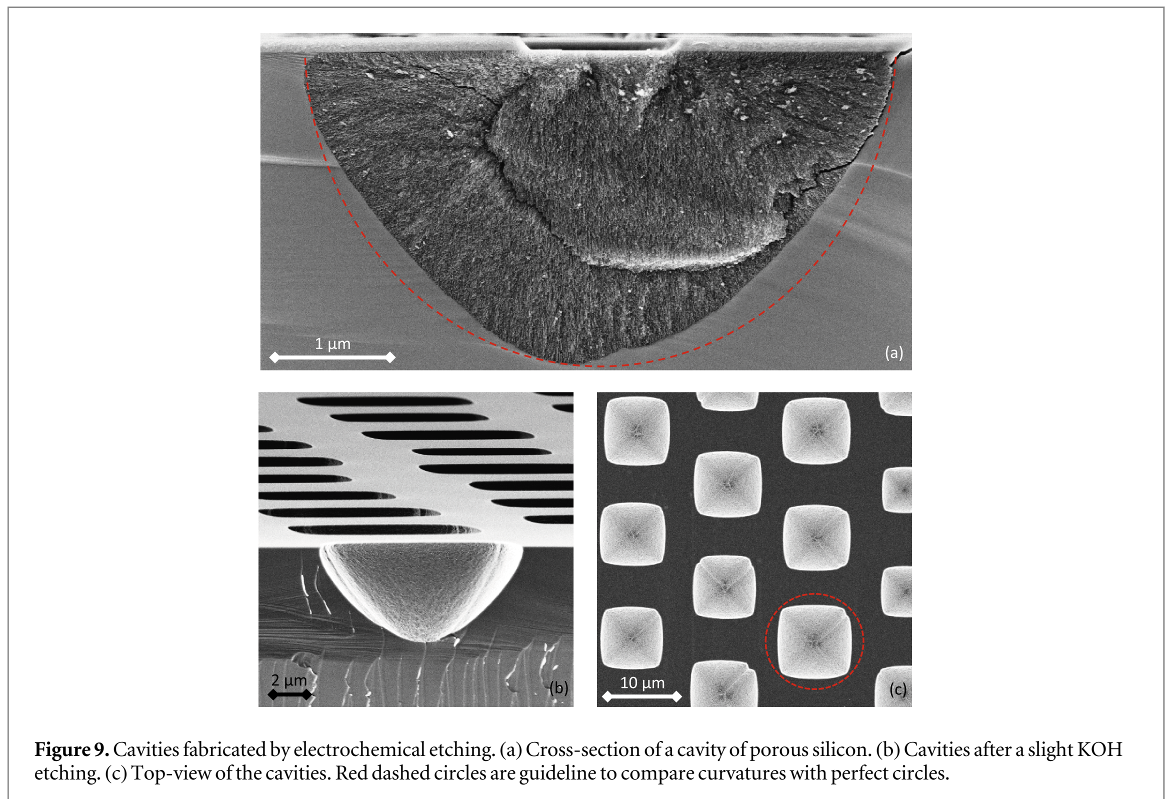

Figure 9. Cavities fabricated by electrochemical etching. (a) Cross-section of a cavity of porous silicon. (b) Cavities after a slight KOH etching. (c) Top-view of the cavities. Red dashed circles are guideline to compare curvatures with perfect circles.

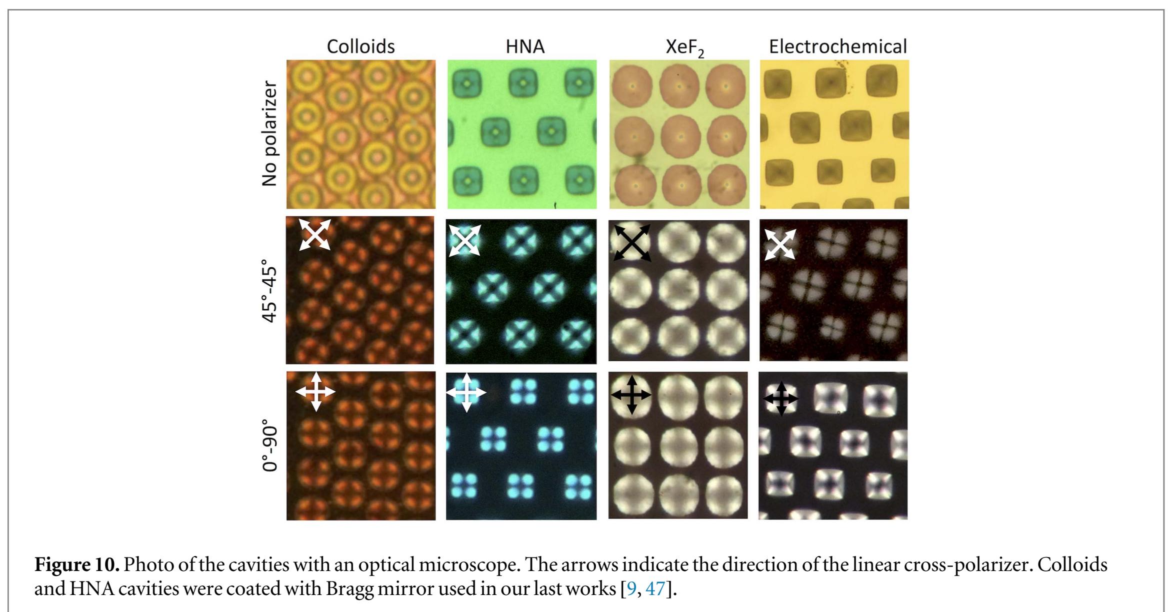

Figure 10. Photo of the cavities with an optical microscope. The arrows indicate the direction of the linear cross-polarizer. Colloids and HNA cavities were coated with Bragg mirror used in our last works [9, 47].

polarization rotation is induced by geometrical rotation due to a double 45°—reflection in hemispherical cavities [9, 17, 32] or due to diffusion because of the surface roughness.

A perfectly hemispherical cavity should exhibit a dark-cross parallel to both perpendicular linear polarizer direction [32]. This is observed in cavities fabricated with colloids or by XeF_2 (figure 10). In the last case, the black-crosses are shaded because of the excessive surface roughness but are still visible. On the other hand, areas between the cavities are black under cross-polarizer because they exhibit specular reflection, which does not induce polarization rotation. The light coming from those surfaces is thus blocked by the cross-polarizer.

The coloured patterns in the case of colloids and XeF_2 are the same, regardless of the cross-polarizer configuration (45°–45° or 0°–90°, figure 10). It indicates that the spherical symmetry of those cavities is perfect. This is not the case with HNA cavities where the 45°–45° configuration gives triangular patterns, linked to the cavity-shape (figure 6(a)). The 0°–90° configuration gives dot-patterns, also due to the cavity-shape (figure 6(c)). The black-crosses here are not fuzzy because the cavity surfaces are highly specular.

Table 1. Comparison between etching methods.

Methods	Fully isotropic	Surface quality	Process complexity	Post smoothing	Main drawback
Colloids	Yes	Specular	4	No	Limited by colloids sizes
HNA	No	Specular	1	No	Sensitive etch rate
XeF_2	Nes	Very rough	2	Yes	Surface roughness
Porous Si	No	Rough	3	Yes	Cavity shape

Optical images of electrochemically etched cavities with the cross-polarizer show that the cavities are distorted as the black cross are not parallel to both perpendicular linear polarizer directions (Figure 10, 45°–45°) and the white dots in a single cavity are not symmetric (figure 10, 0°–90°).

The black crosses are not as visible as in the case of HNA due to the small roughness of the surface and the non-uniformity of the curvature (figure 9(a)) which induces small polarization rotation. Nevertheless, the crosses are more defined that for XeF_2 as the roughness is less important.

4. Discussion

The four methods investigated in this work have pros and cons, which are summarized in table 1.

Cavities fabricated using colloids are perfectly hemispherical with a smooth surface. However, those cavities are not directly made of silicon and their size is limited by the colloids themselves. Moreover, the self-packed method induces a lot of defects and the cavities cannot be easily arranged in something else than a close-packed hexagonal network.

Fabricating cavities with HNA is an easy process but it is not a completely isotropic one. The main disadvantages is the sensitivity of the etch rate with the HNA composition, its temperature and the stirring during the process.

The etch time is thus difficult to predict and coalescence between cavities can happen quickly. On the other hand, the obtained cavity surfaces are highly specular, being thus convenient for optical applications. The isotropicity can still be slightly increased by using ⟨111⟩ silicon wafers [21].

XeF_2 etching is as simple as the HNA etching but needs a post-process to be optically usable. In fact, the fast silicon etching by XeF_2 pulses induces a roughness unsuitable for optical application. However, the cavities are highly hemispherical compared to HNA and electrochemical etching and the XeF_2 process can be controlled *in situ* with an optical microscope.

Cavities made by electrochemical etching also need a post-process to remove the porous silicon in order to reveal the cavities. However, this additional step could be avoided by decreasing the HF content in the electrolyte which would allow the electropolishing regime to take place and prevent formation of porous silicon and thus the presence of surface roughness. This technique also has an anisotropy behavior and lead to squared cavities. The remaining roughness and deformation of the curvature make it so that they are not the first choice for optical applications. The advantages here is that porous photonic structure, such as Bragg mirror or rugate structure, can directly take the shape of a macro cavity or other structures. Complex porous multilayer photonic structures like the *papilio blumei* [20] or the *Hoplia coerulea* [48–51], useful as vapour sensor, can thus be investigated.

All the methods but the colloids allow to arrange the cavities as desired thanks to the optical lithography. Moreover, these 3 methods can also be used to fabricate hemicylindrical cavities [9]. On the other hand, colloids, available in sub-micron size, are more suitable for very small cavities. Indeed, the hemispherical shape takes time to establish with the three other methods because of the size opening in the hard mask and the high etch rate.

5. Conclusion

This work aims at providing an overview of techniques suited to replicate bio-inspired hemispherical structures on planar substrates. While this study intended to produce hemispherical cavities for optical devices their scope is not limited and those cavities can be used in many other applications.

Four processing methods have been investigated: electroplating through a colloidal hard mask, wet isotropic etching with HNA solution, dry isotropic etching with XeF_2 gas and electrochemical etching of the silicon. The four methods gave reasonable results in term of optical applications. Out of these four, HNA results in the best trade off between process complexity and cavity quality. HNA allowed to fabricate cavities with a highly specular surface, compared with XeF_2 and electrochemical etching.

Acknowledgments

Micro-fabrication processes have been done in Wallonia Infrastructure Nano Fabrication (WINFAB) at UCL. J Rasson was supported by a FRIA fellowship (F.R.S.-FNRS).

ORCID iDs

O Poncelet https://orcid.org/0000-0003-3987-6299
J Rasson https://orcid.org/0000-0002-8330-7248
R Kotipalli https://orcid.org/0000-0002-6193-1621
L A Francis https://orcid.org/0000-0003-4683-3916

References

[1] Vukusic P, Sambles J R and Lawrence C R 2000 Structural colour: colour mixing in wing scales of a butterfly *Nature* **404** 457
[2] Lo M-L, Li W-H, Tseng S-Z, Chen S-H, Chan C-H and Lee C-C 2013 Replica of the structural color for papilio blumei butterfly *Journal of Nanophotonics* **7** 073597–073597
[3] Crne M, Sharma V, Blair J, Park J O, Summers C J and Srinivasarao M 2011 Biomimicry of optical microstructures of papilio palinurus *EPL (Europhysics Letters)* **93** 14001
[4] Vukusic P, Sambles R, Lawrence C and Wakely G 2001 Sculpted-multilayer optical effects in two species of papilio butterfly *Appl. Opt.* **40** 1116–25
[5] Liu F, Wang G, Jiang L and Dong B 2010 Structural colouration and optical effects in the wings of papilio peranthus *J. Opt.* **12** 065301
[6] Han Z, Niu S, Zhang L, Liu Z and Ren L 2013 Light trapping effect in wing scales of butterfly papilio peranthus and its simulations *Journal of Bionic Engineering* **10** 162–9
[7] Vigneron J P, Ouedraogo M, Colomer J-F and Rassart M 2009 Spectral sideband produced by a hemispherical concave multilayer on the african shield-bug calidea panaethiopica (scutelleridae) *Phys. Rev.* E **79** 021907
[8] Liu F, Yin H, Dong B, Qing Y, Zhao L, Meyer S, Liu X, Zi J and Chen B 2008 Inconspicuous structural coloration in the elytra of beetles chlorophila obscuripennis (coleoptera) *Phys. Rev.* E **77** 012901
[9] Poncelet O, Tallier G, Simonis P, Cornet A and Francis L A 2015 Synthesis of bio-inspired multilayer polarizers and their application to anti-counterfeiting *Bioinspiration and Biomimetics* **10** 026004
[10] Seago A E, Brady P, Vigneron J-P and Schultz T D 2009 Gold bugs and beyond: a review of iridescence and structural colour mechanisms in beetles (coleoptera) *Journal of the Royal Society Interface* **6** S165–84 (Suppl 2)
[11] Vukusic P, Sambles J R and Lawrence C R 2000 Color mixing inwing scales of a butterfly *Nature* **404** 457
[12] Gaillot D P, Deparis O, Welch V, Wagner B K, Vigneron J P and Summers C J 2008 Composite organic-inorganic butterfly scales: production of photonic structures with atomic layer deposition *Phys. Rev.* E **78** 031922
[13] Summers C J, Gaillot D P, Crne M, Blair J, Park J O, Srinivasarao M, Deparis O, Welch V and Vigneron J-P 2010 Investigations and mimicry of the optical properties of butterfly wings *Journal of Nonlinear Optical Physics & Materials* **19** 489–501
[14] Diao Y-Y and Liu X-Y 2011 Mysterious coloring: structural origin of color mixing for two breeds of papilio butterflies *Optics express* **19** 9232–41
[15] Tam H L, Cheah K W, Goh D T P and Goh J K L 2013 Iridescence and nano-structure differences in papilio butterflies *Optical Materials Express* **3** 1087–92
[16] Deraoui A, Cornet A and Defrance P 2015 Optical properties of bioinspired hemispherical structures *International Journal of Optics and Applications* **5** 187–92
[17] Berthier S, Boulenguez J and Bálint Z 2007 Multiscaled polarization effects in suneve coronata (lepidoptera) and other insects: application to anti-counterfeiting of banknotes *Applied Physics A: Materials Science & Processing* **86** 123–30
[18] Kolle M, Salgard-Cunha P M, Scherer M R J, Huang F, Vukusic P, Mahajan S, Baumberg J J and Steiner U 2010 Mimicking the colourful wing scale structure of the Papilio blumei butterfly *Nat. Nanotechnol.* **5** 511–5
[19] Wang W, Zhang W, Fang X, Huang Y, Liu Q, Gu J and Zhang D 2014 Demonstration of higher colour response with ambient refractive index in papilio blumei as compared to morphorhetenor *Sci. Rep.* **4** 5591
[20] Rasson J, Poncelet O, Mouchet S R, Deparis O and Francis L A 2017 Vapor sensing using a bio-inspired porous silicon photonic crystal *Materials Today: Proc.* **4** 5006–12
[21] Fegely L C, Hutchison D N and Bhave S A 2011 Isotropic etching of 111 SCS for wafer-scale manufacturing of perfectly hemispherical silicon molds *Solid-State Sensors, Actuators and Microsystems Conf. (TRANSDUCERS), 2011 XVI International* (Piscataway, NJ: IEEE) pp 2295–8
[22] Yeh T T, Huang T Y, Tanaka T and Yen T J 2017 Demonstration of a three-dimensional negative index medium operated at multiple-angle incidences by monolithic metallic hemispherical shells *Sci. Rep.* **7** 45549
[23] Lee J K, Choi J C, Jang W I, Kim H-R and Kong S H 2012 Electrowetting lens employing hemispherical cavity formed by hydrofluoric acid, nitric acid, and acetic acid etching of silicon *Japan. J. Appl. Phys.* **51** 06FL05
[24] Bao Y, Zhou F, LeBrun T W and Gorman J J 2017 Concave silicon micromirrors for stable hemispherical optical microcavities *Optics Express* **25** 15493
[25] Bao Y, Cervantes F G, Balijepalli A, Lawall J R, Taylor J M, LeBrun T W and Gorman J J 2016 An optomechanical accelerometer with a high-finesse hemispherical optical cavity *Inertial Sensors and Systems, 2016 IEEE International Symposium on* (Piscataway, NJ: IEEE) pp 105–8
[26] Bae D, Jeon G, Jinnai H, Huh J and Kim J K 2013 Arrangement of block copolymer microdomains confined inside hemispherical cavities *Macromolecules* **46** 5301–7
[27] Lee D, Kim M-H, Bae D, Jeon G, Kim M, Kwak J, Park S J, Kim J U and Kim J K 2014 Arrangement of lamellar microdomains of block copolymer confined in hemispherical cavities having two controlled interfaces *Macromolecules* **47** 3997–4003
[28] Kanungo M, Deepa P N and Collinson M M 2004 Template-directed formation of hemispherical cavities of varying depth and diameter in a silicate matrix prepared by the sol- gel process *Chem. Mater.* **16** 5535–41

[29] Li Y, Cai W, Cao B, Duan G, Sun F, Li C and Jia L 2005 Two-dimensional hierarchical porous silica film and its tunable superhydrophobicity *Nanotechnology* **17** 238
[30] Geng C, Zheng L, Fang H, Yan Q, Wei T, Hao Z, Wang X and Shen D 2013 Fabrication of volcano-shaped nano-patterned sapphire substrates using colloidal self-assembly and wet chemical etching *Nanotechnology* **24** 335301
[31] Sayin M and Dahint R 2017 Formation of charge-nanopatterned templates with flexible geometry via layer by layer deposition of polyelectrolytes for directed self-assembly of gold nanoparticles *Nanotechnology* **28** 135303
[32] Coyle S, Prakash G V, Baumberg J J, Abdelsalem M and Bartlett P N 2003 Spherical micromirrors from templated self-assembly: Polarization rotation on the micron scale *Appl. Phys. Lett.* **83** 767–9
[33] Duan G, Cai W, Li Y, Li Z, Cao B and Luo Y 2006 Transferable ordered ni hollow sphere arrays induced by electrodeposition on colloidal monolayer *The Journal of Physical Chemistry* B **110** 7184–8
[34] Giacchino L and Tai Y-C 2008 Parylene-membrane piezoresistive pressure sensors with XeF_2-etched cavity *In Sensors, 2008 IEEE* (Piscataway, NJ: IEEE) pp 1568–71
[35] Tardan Z and Abdul Halim Z 2011 Comparison of isotropic dry etching process using XeF_2 and anisotropic wet etching process using EDP for microhotplate device *Quality Electronic Design (ASQED), 2011 III Asia Symposium on* (Piscataway, NJ: IEEE) pp 95–9
[36] Cole G D 2012 Cavity optomechanics with low-noise crystalline mirrors *Proc. SPIE* **8458** 845807
[37] André N, Delhaye T P, Al Kadi Jazairli M, Olbrechts B, Gérard P, Francis L A, Raskin J-P and Flandre D 2017 Ultra-low-power SOI CMOS pressure sensor based on orthogonal pMOS gauges *XXII IMEKO TC4 International Symposium and XX International Workshop on ADC Modelling and Testing*
[38] Chen Y, Flader I B, Shin D D, Ahn C H, Ortiz L C and Kenny T W 2017 Fabrication of wide and deep cavities for silicon MEMS devices without wafer bonding *Inertial Sensors and Systems (INERTIAL), 2017 IEEE International Symposium on* (Piscataway, NJ: IEEE) pp 113–6
[39] Vogel N, Goerres S, Landfester K and Weiss C K 2011 A convenient method to produce close-and non-close-packed monolayers using direct assembly at the air-water interface and subsequent plasma-induced size reduction *Macromolecular Chemistry and Physics* **212** 1719–34
[40] Vogel N, Weiss C K and Landfester K 2012 From soft to hard: the generation of functional and complex colloidal monolayers for nanolithography *Soft Matter* **8** 4044–61
[41] Vlad A, Frölich A, Zebrowski T, Dutu C A, Busch K, Melinte S, Wegener M and Huynen I 2013 Direct transcription of two-dimensional colloidal crystal arrays into three-dimensional photonic crystals *Adv. Funct. Mater.* **23** 1164–71
[42] Vogel N, Retsch M, Fustin C-A, del Campo A and Jonas U 2015 Advances in colloidal assembly: the design of structure and hierarchy in two and three dimensions *Chemical Reviews* **115** 6265–311
[43] Robbins H and Schwartz B 1959 Chemical etching of silicon: I. The system, and *J. Electrochem. Soc.* **106** 505–8
[44] Robbins H and Schwartz B 1960 Chemical etching of silicon: II. The system, and *J. Electrochem. Soc.* **107** 108–11
[45] Schwartz B and Robbins H 1976 Chemical etching of silicon: IV. Etching technology *J. Electrochem. Soc.* **123** 1903–9
[46] Zielke D and Frühauf J 1995 Determination of rates for orientation-dependent etching *Sensors and Actuators A: Physical* **48** 151–6
[47] Poncelet O, Tallier G, Mouchet S R, Crahay A, Rasson J, Kotipalli R, Deparis O and Francis L A 2016 Vapour sensitivity of an ALD hierarchical photonic structure inspired by Morpho *Bioinspiration & Biomimetics* **11** 036011
[48] Mouchet S, Su B-L, Tabarrant T, Lucas S and Deparis O 2014 Hoplia coerulea, a porous natural photonic structure as template of optical vapour sensor *In SPIE Photonics Europe* (*International Society for Optics and Photonics*) pp 91270U
[49] Mouchet S R, Tabarrant T, Lucas S, Su B-L, Vukusic P and Deparis O 2016 Vapor sensing with a natural photonic cell *Optics Express* **24** 12267–80
[50] Mouchet S R, Lobet M, Kolaric B, Kaczmarek A M, Van Deun R, Vukusic P, Deparis O and Van Hooijdonk E 2017 Photonic scales of hoplia coerulea beetle: any colour you like *Materials Today: Proc.* **4** 4979–86
[51] Mouchet S R, Van Hooijdonk E, Welch V L, Louette P, Tabarrant T, Vukusic P, Lucas S, Colomer J-F, Su B-L and Deparis O 2017 Assessment of environmental spectral ellipsometry for characterising fluid-induced colour changes in natural photonic structures *Materials Today: Proc.* **4** 4987–97